Vol 1, Issue 2, pages 13-25 ***High School Research Journal***

ENGINEERING A HIGHLY APPLICABLE BASE ISOLATING STRUCTURAL LAYER USING TOPOLOGY OPTIMIZATION AND ADDITIVE MANUFACTURING

Daniel Kim
Half Hollow Hills High School West, New York

ABSTRACT

Current instances of basic and small-scale infrastructure are widely vulnerable to damage from unstable grounds and natural disasters. Unlike many large buildings, structures such as sidewalks and small homes lack any form of base isolation that would reduce the amount of damage they sustain under harsh conditions such as earthquakes, or in common situations such as expanding tree roots and unstable soil conditions. One solution is to develop a design for a simple and easily manufacturable layer of supportive material using topology optimization based on Solid Isotropic Material with Penalization (SIMP). Topology optimization software uses several inputted boundaries, conditions, and parameters, including material properties, maximum area fraction (volume constraint), and penalization factor, and uses them to determine the optimum design for the given problem. Using a computer program called Comsol MultiphysicsR, an optimal two dimensional unit design under constant forces that could be scaled, extruded and multiplied to create a flat layer structure that could properly isolate small scale superstructure from unstable grounds was investigated. Our intention was to develop a design for a form of base isolation that could be easily-applied to a variety of different situations, adjusted to each one, and utilize either prevalent or contemporary methods of manufacturing such as additive manufacturing to create. The model's maximum area fraction was adjusted and analyzed in order to determine the most efficient use of material, and most optimal design. While a basic structure is generated, further studies are necessary to determine the better use of materials type and size as well as improve upon the design and manufacturing process. The application of this technology would lead to greater structural stability in small-scale infrastructure, reduce the need for maintenance, lower costs, and provide safer environments for people to travel and live in.

Keywords: Topology optimization; Additive manufacturing; 3-D printing; Small scale infrastructure; Base isolation; Solid isotropic materials with penalization (SIMP).

INTRODUCTION

Today, infrastructures' need for protection against earthquakes and unstable grounds continues to be a problem, particularly in third world countries and urban areas. Common solutions today revolve around the development of base isolation technology that has now become a popular option since its conception more than 100 years ago [1]. Base isolation typically creates a flexible connection between a structure and its foundation that allows them to move separately from one another and reduce the impact of seismic forces on the structure [2]. However, there is a lack of development for base isolation technologies for small scale infrastructure such as sidewalks and small homes which results in billions of dollars in damage in the United States alone in the case of earthquakes, and catastrophic events in countries such as Haiti where the necessary repairs are unfunded and thousands are affected [3, 4]. Additionally, mundane damages caused by unstable grounds, and street tree roots to sidewalks, roads, and home foundations result in a multi-million dollar problem in the United States [5]. Although products and services such as root barriers and root pruning exist to combat these problems, they are often only effected for a limited period and/ or restrict the tree's growth leading to unhealthy developments [6, 7]. Our proposed solution is to design the structure for a layer of solid material beneath such structures that can help to isolate them from both smaller seismic activity and unstable grounds and tree roots. Ideally, this layer would provide a degree of conformity to deal with the ground protrusions and tree roots as well as negate some of the seismic damage to the supported infrastructure, but still maintain enough structural integrity to withstand the static forces placed on it on a day-to-day basis without fail. This work proposes the use of SIMP based topology optimization in order to create the design for the layer and also the use of additive manufacturing (3D printing) in order to manufacture the proposed structure when it becomes economically viable.

Base Isolation

Also known as seismic base isolation or base isolation systems, base isolation helps protect a given structure from earthquake forces [8]. In general, the system attempts to reduce the amount of interaction a superstructure has with its substructure using several structural elements so that the superstructure, integrity can be maintained despite any shaking the substructure may experience from the ground [9]. Base isolation does not guarantee a building or structure to be earthquake proof, rather its application simply raises its seismic performance and sustainability. Both describe the structure's ability to continue its basic functions, including safety and serviceability, during and after an earthquake, with safe being described as if the structure does not threaten the lives of those inside or around it by collapsing and serviceability being if it can still perform its regularly designed functions [10].

Base isolation systems are made up of two parts, isolation units with isolation components and isolation units without isolation components. Isolation units are the fundamental parts of a base isolation systems that are used to decouple the superstructure from its substructure, while isolation components are merely connections that provide no effect on their own [2]. The isolation units with isolation components come in two types: bearings, which protect against lateral movements caused by earthquakes, and dampers, which absorb or dissipate the energy stored in the base [9]. These bearings, as seen in Figure 1, are commonly either lead-rubber bearings or spherical sliding bearings which both provide limited vertical movement and are free or flexible in the horizontal direction. Lead-rubber bearings work by allowing a building to maintain its shape and its vertical position while vibrating back and forth during an earthquake. The vibrations are also lengthened by the bearing which reduces the acceleration of the building and prevents the structure from experiencing harsher changes in speed. Meanwhile, spherical sliding bearings work by allowing the building to slide freely around the curved surface of the bearing's foundation and limits horizontal movement based on the large amount of force necessary to move vertically on the foundation [11].

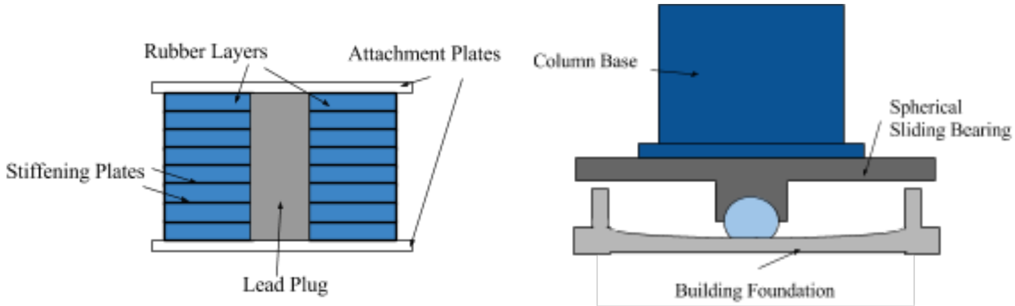

Figure 1 shows a standard example of a static lead-rubber bearing on the left. As shown, this bearing's attachment plates and stiffening plates maintain a parallel relationship to one another so that the flexible rubber layers and lead plug can shift to allow for a significant range of horizontal movement to counter violent seismic activity. The right image shows an example of a spherical sliding bearing. The curved foundation and large force it takes to move vertically up it would cause the building rock slowly until it resettles in the middle of the foundation.

The proposed project is unable to make effective use of these designs because of sidewalks' and streets' extensive area, direct layering over their base and subgrade, and relatively lower density to a building. Smaller homes and buildings may be able to make some use of these designs, but their lower weights and size would reduce their effectiveness. So, the project's concept will design a wide structure that allows the supported structure's horizontal movement by utilizing a flexible material, similar to what a lead-rubber bearing would accomplish, and will disperse the force of the building over an even wider area than an isolation bearing allowing it to easily maintain its own integrity.

Topological Optimization Software and Three-Dimensional Printing

Engineering has always been the application of mathematic and scientific knowledge in order to design, develop, and analyze structures, tools, materials, and systems [12]. However, modern technology allows researchers to become significantly more efficient and capable of creating optimized solutions to more problems and scenarios. A major source of productivity has been the result of developing machines and programs such as 3D printers and topology optimization software which helps reducing the need for iterative design processes that consume a massive amount of time and resources in order to conceive, prototype, and develop new ideas [13, 14]. Additionally, these developments have allowed industries to make more customizable and specifically tailored products and structures that conform to the needs and wants of consumers and infrastructure [13]. The technology is highly adaptable and has found a wide use in small manufacturing industries as well as larger businesses such as aerospace [15].

Topology optimization takes a mathematical approach to finding the distribution of material within a design domain for a given problem. In general, topology optimization is based on methods of moving asymptotes, genetic algorithms, optimality criteria methods, level-sets methods, and topological derivatives that take into account of a limited number of elements [16]. Typically, used during the concept level of the design process, and allows users to quickly develop a model that is optimized for performance and manufacturability [14]. This helps to bypass the need to make timely and costly intuitive design iterations, and create more efficient and effective models.

Topology optimization problems follow a generic problem expressed as:

$$\min_{\rho} \int_{\Omega} \phi(\rho)\, \mathrm{d}\Omega$$

Which describes the interaction between the objective functional ($\int_{\Omega}\Phi(p)d\Omega$), design space(Ω), discrete selection field (p), design constraints, and governing equations. Here, the goal is to minimize the objective functional which will be the strain energy of the structure for this study. The design space designates the area or volume in which the design is allowed to exist and is dependent on the structure's purpose and manufacturing constraints. The discrete selection field runs through points in the design space and designates whether each one will adopt a value of one or zero, and the governing differential equation dictates the physics involved with the structure being made [17].

The general problem described above requires discrete optimization over each point in the given domain area, but since that is currently unobtainable, it is assumed that p continuously varies over the domain (0,1) and is solved based on a specific number of elements made by the meshing of the design. A common method of doing this is the Solid Isotropic Material with Penalization or SIMP method which interpolates the Young's modulus to a scalar selection field based off of a power law $E = E_0 + p^n E_1$. This essentially results in the optimization of the microstructure at all points in space and guarantees the minimization of the objective function [18].

In addition to topological optimization, 3D printing helps to expedite the design and manufacturing phase of production. Designs generated by topology optimization can be realized as 3D models and printed out so that they can be tested or analyzed for any flaws. Recent years have seen a massive amount of innovation that allows 3D printers to be more readily available to industries and consumers with a wider range of functions including different material types, intricate and detailed productions, and lower manufacturing costs [19].

Through the use of topology optimization, a simple and widely applicable unit design will be generated. 3D topology optimization proves to be significantly more complicated and intensive than 2D printing, and a simple repeatable design that could easily be realized was a primary objective. So, a 2D topology optimization was carried out with the intention to later extrude the design in order to create a 3D structure that could be printed. Ideally the design would be scaled, extruded to a given length, and multiplied side by side in order to create a base isolating layer that could support small-scale infrastructure.

Since the shape and success of the design is dependent upon minimizing the objective function, which in this project will be the strain energy of the structure, under the design constraints, the research goal is to discover a maximum area fraction and design domain that efficiently reduces the strain energy. A maximum area fraction of 1, although an inefficient use of material, would provide the least amount of strain energy as the atoms would physically have less open area to rearrange themselves and begin to store strain energy, a form of potential energy [20]. So, the smallest maximum area fraction that allows for a strain energy within a reasonable range of that of a fully solid structure would be ideal. So, based on the general exponential increase of a stress-strain curve and because more massive objects experience less stress from the same force, one could expect logarithmically decreasing returns on using a greater maximum area fraction [21]. So, one could can theorize that design with a maximum area fraction from 0.5 to 0.6 will see the greatest returns and provide the most efficient design for supporting small-scale structures.

METHODS

Topology optimization in Comsol MultiphysicsR is based on a series of inputted boundary conditions describing the problem and determines the best shape for the structure. The program uses the total strain energy of the structure as its criterion for optimality since the strain energy is equitable to the work done by an applied force. So the reduction of the strain energy also reduces the displacements caused by these forces which minimizes the conformity of the structure and results in the maximization of the structure's stiffness. On the other hand, the system also has to take into account for the total available mass for the structure, which it establishes as an upper bound that restricts the resulting structure.

Topology optimization is also required to be binary, meaning each point on the structure is determined to be either solid or void. Any alternative would be implausible since material would either exist or not exist in a given location. Additionally, "checkerboard" patterns in the structure must also be avoided for practical reasons. The SIMP penalization method follows the optimization problem:

$$E(x) = \rho_{design}(x)^{\rho} E_0$$

$$x \,\varepsilon\, \Omega$$

Here, the artificial density, ρ_{design} , acts as a control variable as the stress tensor is treated as a
function of the Young's modulus E_0 . For numerical reasons, the stiffness of the structure must also not be completely void in any part of the model. So the density parameter is given a range of $10^{-9} \leq \rho^{p} \leq 1$. The exponent p which must be greater than 1 is a penalty factor causes any transitional densities contribute less stiffness in comparison to their weight cost.
When the maximum area fraction, γ , of the domain area, A, is described, the SIMP penalization method forces ρ_{design} towards either bound. This causes any increase in p to create a more detailed solution as described by;

$$0 \leq \int_{\Omega} \rho_{design}(x) d\Omega \leq \gamma A$$

However, the design should avoid having excessive fine detail, as that would compromise the final design's reliability.

Another consideration is to smooth out the solution and remove unwanted details caused by the mesh resolution by implementing a form of regularization. The program used does this through a series of mesh refinements and gradient penalties to the design variable. The total variation of the design variable can be described by the integral of the squared norm of the gradient of ρ_{design} . Additionally, the gradient size is inversely proportional to the mesh element size, while the area is proportional to it. As expressed by:

$$\frac{h_0 h_{max}}{A} \int_{\Omega} |\nabla \rho \ (x)^2| d\Omega$$

an acceptable penalty term that isolates the solution from the mesh resolution is achieved, where the initial mesh size, h $_0$, which determines the solution's detail size and the current mesh size, h_{max}, are at a given level.

The strain energy must also be normalized in order to balance the penalty term against it, particularly when the penalty term may be on the order of 1. This is done by solving the structural problem based on an initial homogeneous $\rho_{design} = \gamma$ and then dividing the strain energy by the total strain energy, W_{s0}, for the previous structure. Finally, the objective and the penalty term must be balanced against each other, which results in the final composite objective function [22];

$$f = \frac{(1-q)}{W_{s0}} \int_{\Omega} W_s(x) d\Omega + q \frac{h_0 h_{max}}{A} \int_{\Omega} \left| \nabla \rho_{design}(x)^2 \right| d\Omega$$

A structure with the parameters shown in Figure 2 were finally chosen.

Name	Value	Description
h_0	.0125	Initial mesh size
h_{max}	.0125	Current mesh size
p	5	SIMP penalization factor
q	.25	Regularization factor
gamma	.5	Maximum area fraction
domainArea	1^2[m^2]	Area of design domain
W_{s0}	1 †	Reference objective value
Young's modulus	2.9e9[Pa]	Young's modulus

† Later updates to 64.7 before the optimization is started.

Figure 2 shows the parameters used for the topology optimization of the structure.

and given boundaries were expressed as shown in Figure 3.

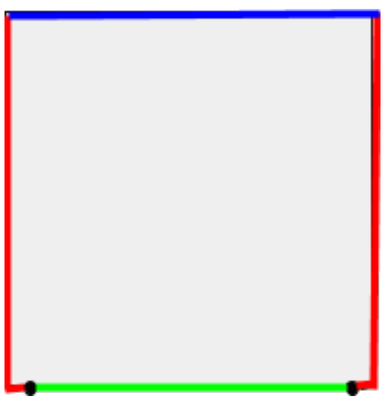

Figure 3 displays the utilized boundaries with red lines indicating rollers, the blue line indicating a -100 kN boundary load in the y-axis, and green lines indicating a +100 kN boundary load in the y-axis.

Several probes were also established to gather information concerning the structures normalized strain energy(J/m), gradient penalty (m^2), mass utilization, total elastic strain energy (J), and objective value (J/m). Additionally, the software was run multiple times with different parameters including different maximum area fractions ranging from 0.2 to 1.0, and a 2x1 m^2 design area after determining a desirable max area fraction to analyze its effects on the previous, and compare the results[22].

After a final design was chosen, a 3D model was also printed to demonstrate the validity of the technology. Using the image of the topology produced by Comsol MultiphysicsR, a black and white images was generated and extruded to create a 3D model that was later printed. All images and graph data was generated using Comsol MultiphysicsR.

RESULTS AND DISCUSSION

Once the optimization software completed determining the best shape for the structure, images are given depicting the final von Mises stress (N/m^2) stress, more importantly the topology, and data for each of the probes established earlier.

Design Number	Maximum Area Fraction	Normalized Strain Energy(J/m)	Gradient Penalty (m2)	Mass Utilization	Total Elastic Strain Energy (J)	Objective Value (J/m)
1	0.2	1.7362	0.071875	0.9807	112.33	1.3022
2	0.3	0.26541	0.098751	0.99937	17.172	0.19906
3	0.4	0.13156	0.062213	0.99812	8.5121	0.098672
4	0.5	0.083544	0.050538	0.99931	5.4053	0.062658
5	0.6	0.062715	0.035149	0.99985	4.0577	0.047037
6	0.7	0.049241	0.02079	0.99993	3.1859	0.036931
7	0.8	0.04159	0.0079008	0.99989	2.6909	0.031192
8	0.9	0.037104	3.41E-04	0.99998	2.4006	0.027828
9	1	0.022502	1.2266E-33	1.00000	1.4559	0.016877

Figure 4 shows the data collected from the probes established during each run of the optimization software in order to compare the effects of changing the maximum area fraction.

As expected, the strain energies, gradient penalty, and objective value became logarithmically smaller as a greater amount of mass was available for use to support the structure and it approaches the physical limit of filling the entire area with material. There are significant drop offs greater than 0.02 J/m in normalized strain energy from a maximum area fraction of 0.2 to .6 that significantly increase the structure's stiffness. However, after 0.6 to 0.7 any change in area fraction is much less impactful, less than 0.01 J/m and becomes a relatively inefficient use of mass. This drop off is seen in Figure 5 where the curve quickly begins to level out after 0.7

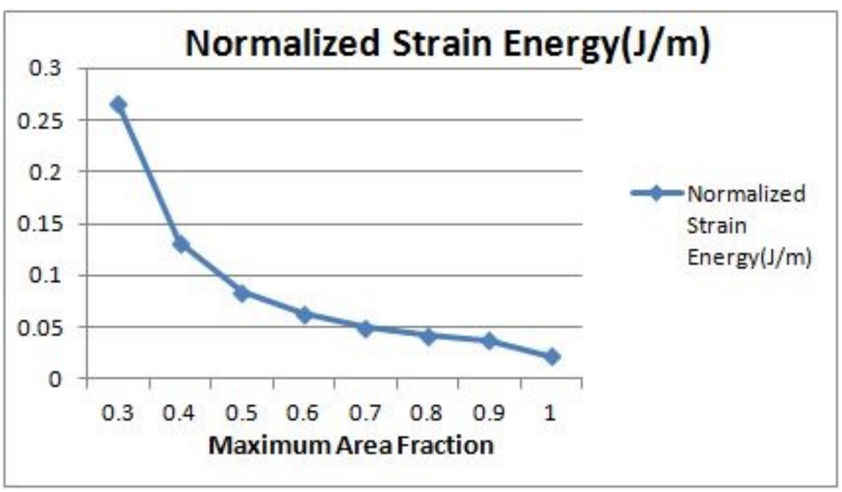

Figure 5 shows the normalized strain energy and its logarithmic decrease as the maximum area fraction increases. The slope is steep prior to a maximum area fraction of 0.6 and significantly decreases after a maximum area fraction of 0.7

A similar pattern is seen with the gradient penalties, and object values.
In addition to the raw information gathered from the probes, the images of each of the generated model's topology makes their relative strain energies visually apparent. Since a given location cannot be completely void for numerical reasons, most points are given a value at the extremes of the density parameter with some areas being intermediate. Depending on the user's preference, the final design can constitute of as much or as little of the intermediate areas but at the cost of reliability.

The topology of design 1 seen in Figure 6 is nearly non-existent which explains its significantly higher strain energy, while the structure of design 2 is significantly thicker than that of design 1's and has more substantial connections to both the top and bottom of the design area where it would interact with the ground and the structure it is helping to isolate.

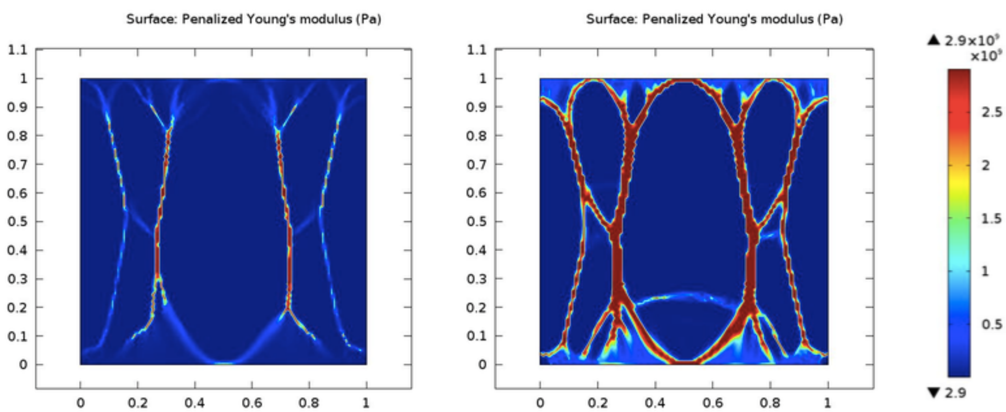

Figure 6 depicts the topologies of design 1 on the left and design 2 on the right.

Design 3 continues to make the structure more substantial in Figure 7, and creates more intermediate areas on the top and bottom of the design area. Finally, design 4 begins to completely fill in "empty" areas between the tendrils of the structure on the top and bottom of the design area, and also begins the development of a central column.

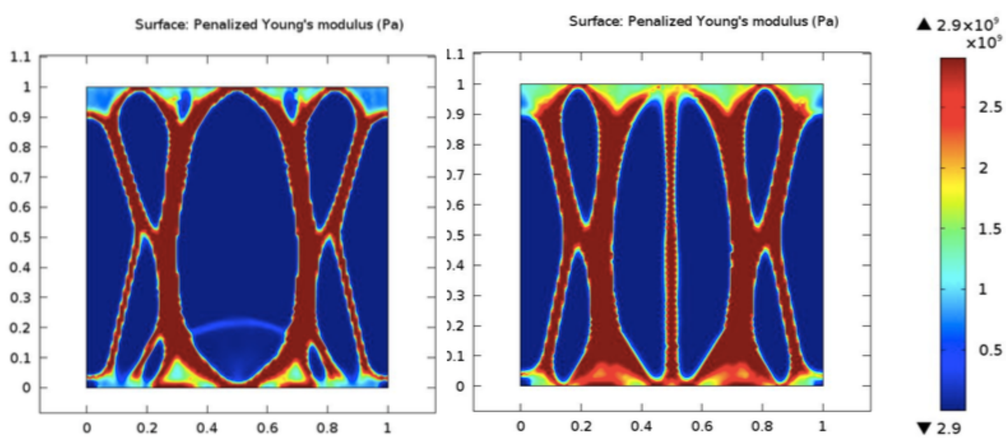

Figure 7 depicts the topologies of design 3 on the left and design 4 on the right.

Designs 5 and 6 shown in Figure 8 are the most prominent as the areas near the top and bottom of the design area are predominantly filled and connected to the rest of the structure. Additionally, the center and side supports appear more fleshed out unlike the previous designs that were more weblike and spindly. These designs also had the lowest strain energies while maintaining a relatively low maximum area fraction. Although, design 5's maximum area fraction could still be higher to achieve a significant difference in strain energy, whereas design 7's maximum area fraction is borderline excessive and inefficient.

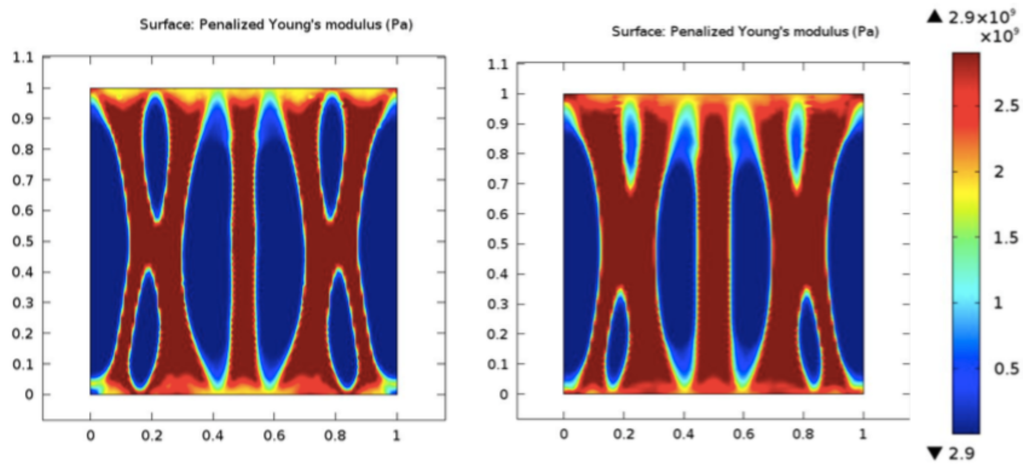

Figure 8 depicts the topologies of design 5 on the left and design 6 on the right.

Finally, designs 7 and 8 have the completely opposite problems of designs 1-4 because they have substantially low strain energies, but their immense maximum area fractions of 0.8 and 0.9 are excessive and inefficient uses of material. Seen in Figure 9 nearly the entire domain area is filled and the designs transition into low detailed columns or just a single thick column.

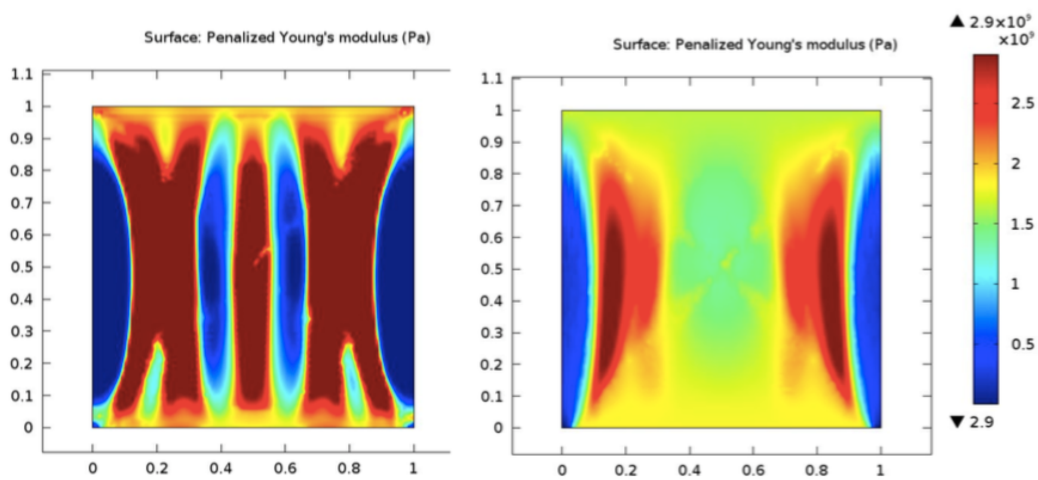

Figure 9 depicts the topologies of design 7 on the left and design 8 on the right.

Based on the strain energies and topologies of each of the designs, it seems that a design with a maximum area fraction between 0.6 and 0.7 would be most optimal. So, a design was generated with a 0.65 maximum area fraction as well as a design with a 0.65 maximum area fraction and a 2x1 m^2 domain area. After determining that a design with a 0.65 maximum area fraction and a 1x1 m^2 domain area was the best, a 1x1 m^2 design with a 0.65 maximum area fraction was generated with a finer mesh size of 0.0025 rather than 0.125. The same data was collected and is shown in Figure 10.

Design Number	Maximum Area Fraction	Iteration Number	Normalized Strain Energy(J/m)	Gradient Penalty (m2)	Mass Utilization	Total Elastic Strain Energy (J)	Objective Value (J/m)
11	.65	23	0.0561	0.027774	0.99982	3.6297	0.042075
12*	.65	25	0.12033	0.038131	0.99902	7.7851	0.090245
13 †	.65	26	0.050045	0.0052649	0.9999	3.2379	0.037533

* Design with a 2x1 m^2 domain area

† Design with a 0.0025 mesh size

Figure 10 shows the data collected from the probes established during each run of the optimization software in order to compare the effects of changing domain area and mesh size.

In comparison to figure 4's table, design 11 has an expected strain energy between that of designs 5 and 6 and boasts a healthy low strain energy and relatively low use of material for its stiffness. Also, design 12 had a significantly greater strain energy with its design area of 2x1 m^2 than design 11 with a design area of 1x1 m^2. This helped to prove that despite using the same maximum area fraction, a smaller unit design will provide a more reliable structure overall. On the other hand, design 13 saw a reduction in its strain energy with its finer mesh size of 0.0025 over design 11 with a mesh size of 0.0125, although the difference is extremely minimal. Once again the topological designs help explain the reason for these differences visually.

Starting with design 12's topology in Figure 11, one could see that it is less organized than many of the other designs as it has an extensive amount of oddly bent individual columns and strange protrusions alongside the fourth most outer columns. In comparison to the "X" shaped columns common to all of the other designs, design 12's topology is inherently weaker and makes poor use of the available mass.

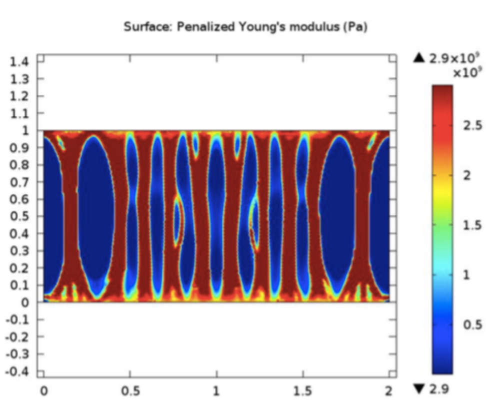

Figure 11 depicts the topology of design 12.

Design 11 and 13 share the same structure shared by all the 1x1 m^2 designs but achieve an optimal structure that is not thin and weak, nor thick and excessive. As shown in Figure 12, Design 13 shows a much more well defined structure with significantly less intermediately defined area surrounding the design, but has also developed extraneous defects along the middle column and an asymmetrical design on the lower half.

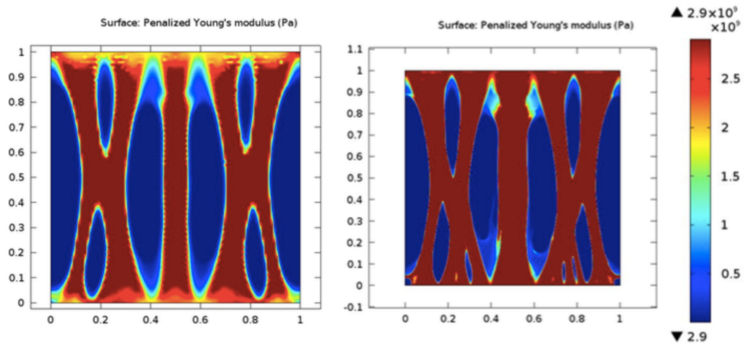

Figure 12 depicts the topologies of design 11 on the left and design 13 on the right.

Using design 13’s image of its topology, a black and white image was generated, scaled and extruded 2 cm to create a plastic 3D model that was later printed using a Flashforge Dreamer 3D printer in the span of about 4 to 5 hours. The model helped to demonstrate the potential application of additive manufacturing in quickly producing abstract structures with little to no time between designing and manufacturing.

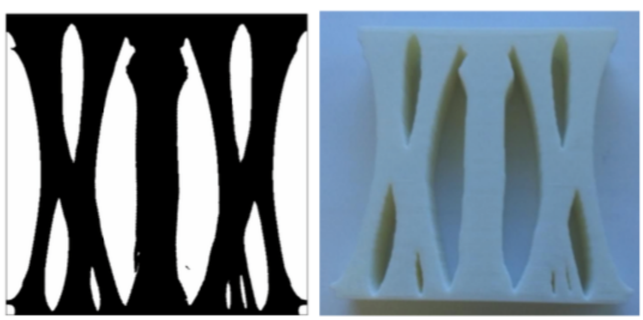

Figure 13 shows the black and white image generated from design 13’s topology on the left and on the right shows the finished three-dimensional model made from the extruded design.

CONCLUSION

The design utilizing a maximum area fraction of .65 seemed to be the best choice while balancing the minimization of the structure’s strain energy and use of material. Thus the hypothesis was not supported that the optimum design would be found using a maximum area fraction of 0.5 to 0.6. Although the strain energy difference between increasing area fractions logarithmically decreased, differences from 0.5 to 0.6 and 0.6 to 0.65 resulted in relatively large changes in strain energy of more than 0.02 (J/m). The use of topology optimization allowed for the swift collection of data and information concerning the design and efficiency of those designs, and could produce more accurate results for a problem using a more specific and well defined set of parameters and boundary conditions. Additionally, the use of 3D printing proved to be a convenient and efficient method of producing a tangible example of the product in contrast to contemporary subtractive methods which would have required a greater amount of time and resources to set up and function. Although, the technology is still limited by its relatively high costs, lack of infrastructure in industries, and limited materials.

Applications

The application of this type of design is primarily in supporting small-scale architecture and isolating them from unstable ground conditions and minor seismic forces. As a unit design, it can easily be scaled to match a given situation, whether it be a small home or sidewalk, and be extruded and repeated to create a structural later that can fill the necessary area. In large cities and suburban areas, sidewalks and small homes can be isolated and protected from unstable ground and intrusions such as tree roots that regularly force up against them. This regular creation of unsafe, or at least inconvenient and costly damages to private and public properties, could be avoided by having a layer of material that absorbs the forces or at least helps to reduce the impact on the structure. Also, in places where earthquakes are rampant and materials to build stable homes are scarce, this design could potentially provide a cheaper method of establishing some form of base isolation depending on the material used.

Future Research

This research was performed using a generalized sat of parameters and boundary conditions in order to create a broadly applicable design that may not be entirely optimal for every given situation. One extension of the research would be to develop designs with specific problems, such as just sidewalks or small homes, in mind and adjusting the conditions those that each one would require. If the resources and time are available, the use of three dimensional topology optimization would also be a worthy endeavor to create a much more complex design. More importantly, however, would be the investigation of the optimal types and use of material according to the design. Topology optimization is concerned with the shape of the design and only accounts for the young's modulus of the structure in this case. In order to come to a final solution or physical structure, simulation, testing, and analysis concerning the materials it is made up of would have to be done separately. Finally, testing the creation of larger instances of the design using 3D printing and other materials would be useful to test the current limitations and observe what would need to be developed to eventually make them viable option options of manufacturing.

References

1. Buckle, Ian G., and Ronald L. Mayes. "Seismic isolation: history, application, and performance-a world view." *Earthquake spectra* 6.2 (1990): 161-201.
2. Pressman, Andy. *Architectural graphic standards*. John Wiley & Sons, 2007.
3. Kilesen, Kevin L. "The Economics of Natural Disasters." *The Economics of Natural Disasters*. N.p., n.d. Web.
4. "Haiti earthquake of 2010". *Encyclopædia Britannica*. *Encyclopædia Britannica Online*. Encyclopædia Britannica Inc., 2016. Web. 17 Sep. 2016 <https://www.britannica.com/event/Haiti-earthquake-of-2010>.
5. McPherson, E. Gregory, and Paula P. Peper. "Costs of street tree damage to infrastructure." Arboricultural Journal 20.2 (1996): 143-160.
6. Lippi, Chuck. "Blog." The Use of Root Barriers to Protect Infrastructure from Roots. N.p., n.d. Web. 17 Sept. 2016.

7. Zahner, Robert, and Norbert V. DeByle. "Effect of pruning the parent root on growth of aspen suckers." *Ecology* 46.3 (1965): 373-375.
8. Ramallo, J. C., E. A. Johnson, and B. F. Spencer Jr. "“Smart” base isolation systems." *Journal of Engineering Mechanics* 128.10 (2002): 1088-1099.
9. EFILOGLU, Mustafa. "UNDERSTANDING THE CONCEPT OF BASE ISOLATION." (n.d.): n. pag. *Http://www.manchester.ac.uk/*. 24 July 2013. Web.
10. Shustov, Valentin. "Seismic Fitness: On Some Features of Earthquake Engineering." (n.d.): n. pag. *NEEShub*. Web.
11. "Base Isolation – Earthquake Resistant Design Techniques." *21st Century Builder*. N.p., 08 Jan. 2014. Web. 18 Sept. 2016.
12. "engineering". *Encyclopædia Britannica*. *Encyclopædia Britannica Online*. Encyclopædia Britannica Inc., 2016. Web. 17 Sep. 2016 <https://www.britannica.com/technology/engineering>.
13. LI Xiao-dong1, lxd_8111@163.com, and Fan1 Zhao. "3D Printing Technology Impact On Development Of Industrial Design." *Key Engineering Materials* 693.(2016): 1901-1904. *Applied Science & Technology Source*. Web. 17 Sept. 2016.
14. Eschenauer, Hans A., and Niels Olhoff. "Topology optimization of continuum structures: a review." *Applied Mechanics Reviews* 54.4 (2001): 331-390.
15. Sobieszczanski-Sobieski, Jaroslaw, and Raphael T. Haftka. "Multidisciplinary aerospace design optimization: survey of recent developments." *Structural optimization* 14.1 (1997): 1-23.
16. Bendsoe, Martin Philip, and Ole Sigmund. Topology Optimization: Theory, Methods, and Applications. N.p.: Springer Science & Business Media, 2003. Google Books. Springer Science & Business Media, 1 Dec. 2003. Web.
17. Sigmund, M.P. Bendsùe O. "Material Interpolation Schemes in Topology Optimization." *Giref.ulaval*. N.p., 1999. Web.
18. Pedersen, N.L. "Maximization of Eigenvalues Using Topology Optimization." *SpringerLink*. N.p., 10 June 1999. Web. 18 Sept. 2016.
19. Berman, Barry. "3-D printing: The new industrial revolution." *Business horizons* 55.2 (2012): 155-162.
20. Smith, Michael B., and Jerry March. March's advanced organic chemistry: reactions, mechanisms, and structure. John Wiley & Sons, 2007.
21. Roylance, David. "Stress-strain curves." Massachusetts Institute of Technology study, Cambridge (2001).
22. "Topology Optimization of an MBB Beam." (n.d.): n. pag. *Comsol*. COMSOL Multiphysics®. Web.